RESEARCH PAPER

Computational Analysis on Elastic-Plastic Fracture of Al/B_4C and Al_2SiO_5 Hybrid Metal Matrix Composites

Puneeth Niranjan[1], Gangarekaluve J Naveen[1,*], Vishwanath Koti[1], Nitrahalli D Prasanna[2], Litton Bhandari[3], Javaregowda Satheesh[4], Parthasarathy Sampathkumaran[5]

** gj_naveen@yahoo.co.in*

[1] **Research Scholar, Department of Mechanical Engineering, Visvesvaraya Technological University, Belagavi, Karnataka, India,**

[2] **Department of Mechanical Engineering, Ramaiah Institute of Technology, Bengaluru, Karnataka, India**

[3] **Department of Materials Science and Engineering Engineering, Indian Institute of Technology Gandhinagar, India**

[4] **Department of Mechanical Engineering, S J B Institute of Technology, Bengaluru, Karnataka, India**

[5] **Department of Mechanical Engineering, Sambhram Institute of Technology, Bengaluru, Karnataka, India**

Received: October 2021 Revised: December 2021 Accepted: January 2022

DOI: 10.22068/ijmse.2507

Abstract: *In this study the hybrid composites were developed using the stir casting technique as per Taguchi's L9 orthogonal array. Hybrid composites were fabricated using Aluminium Al6082 as the base material and reinforced with the combinations of reinforcements Al_2SiO_5 and B_4C at three levels (4, 8, and 12%). The developed composites were analyzed for micro- structurally and mechanical tests were performed as per ASTM standards. The microstructural analysis was done using an optical microscope and scanning electron microscope while compositional studies were done using X-ray diffraction and EDAX analysis. Mechanical tests such as tensile, impact, and flexural were conducted and their damage assessment was done using a scanning electron microscope. The fatigue characteristics like high cycle fatigue and fatigue crack propagation were studied both experimentally and numerically. The experimental data and numerical modeling analysis data obtained for the hybrid composite system, agreed with each other.*

Keywords: *Boron Carbide (B_4C), Aluminium Silicate (Al_2SiO_5), X-ray diffraction, Scanning electron microscope (SEM).*

1. INTRODUCTION

Aluminum metal matrix composites are the recent and advanced metal matrix composites (MMC) that possess superior mechanical, thermal, and chemical properties. The need for lightweight and superior properties has been satisfied by the development of advanced aluminum metal matrix composites. Also, it is to be noted that a wise choice of reinforcements, processing techniques, and parameters have made a good influence on the development of Aluminium composites having superior properties. Furthermore, processing techniques should be made easy, less expensive tooling required, easy to access, and less requirement of highly skilled manpower. Such processing methods are quite helpful for the industries to adopt and produce composites of the required size and shape on a large scale. Liquid metallurgy technique such as stir casting has proven to be highly effective for the processing of aluminum-based composites among the various routes. Stir casting has got all the potential to mass production of automotive components, aerospace components, etc. [1, 2]. However, there are a large number of variables and factors that need to address carefully for the selection of appropriate processing parameters to yield a mass production [3, 4]. Artificial neural networks, the Taguchi method, and genetic algorithms are the few well-known techniques that are used for process optimization to get better mechanical and tribological properties [5, 6]. In the current study, process parameters were optimized and fatigue and fracture analyses were done using both experimental and computational methods to predict the failure of the composites. Before the conduction of experimental work due to its economics and complexity, a new evaluation phase like computational with NASTRAN, ANSYS for fatigue life evaluation would be an added advantage. Test parameters involved in manufacturing hybrid MMC's via stir casting involve numerous such as stir speed, stir speed,

[DOI: 10.22068/ijmse.2507]

the volume fraction of reinforcements need to be optimized as well. Design of experiments using the ANOVA approach is one such tool to create and obtain plots for fracture resistance properties. Keeping all the above points in view, the current progress envisages the study of Al MMC's involving ANOVAs model obtained through the design of experiments. The process parameters were optimized to evaluate fatigue properties using fatigue apparatus and the properties were in comparison with hardness, microstructure, and also graph indicating deflection vs. load Plot. The boron carbide as reinforcement chosen based on the basic mechanical properties especially elastic modulus to match with the Aluminium matrix, namely Al6082 is shown in Table 1 and Properties of particulate reinforcement is shown in Table 2.

2. EXPERIMENTAL PROCEDURE

Metal hybrid composites were fabricated using moderate strength Aluminium alloy such as Al6082 which was chosen as matrix material. This alloy is well known for its medium strength, corrosion resistance, machinability, and good weldability. Furthermore, Al8062 matrix was reinforced with B_4C and Al_2SiO_5 ceramic particles and their various attributes that are tabulated in Table 3.

The average particle size of B_4C and Al_2SiO_5 ceramic particles were found to be 63 and 25 µm respectively. While fabricating the hybrid metal matrix composites, the weight % of Al_2SiO_5 was kept constant and B_4C content was varied from 4% to 12% as shown in Table 3. Also, Table 3 shows the designation used for types of Al6082 hybrid composites with a different weight percentage of B_4C and Al_2SiO_5 ceramic particles and would be used in the later section of the present work. Table 4 shows the processing parameters with respective levels.

Table 5 shows the nine different composites that were developed with different parameters and at different levels.

The effect of these parameters on tensile strength and fracture toughness of the composite was analyzed using analysis of variance (ANOVA). The design of experiments viz., Taguchi method is applied to study the response variable using the variations due to uncontrollable parameters. The principle of "the larger–the better" is applied to the responses, which are regarded as quality attributes. Standard Taguchi's method with L9 orthogonal array was adopted for, statistical analysis. The orthogonal array helps study the effect of various control factors and provides optimal solutions. The experimental results obtained were transformed to Signal-to-Noise ratio (S/N) which is calculated by the following expression,

$$S/N = -10\log \{1/n \sum n_i=1\ 1/Y_i2\} \quad (1)$$

Where n is the number of experiments and Y_i is the measurement result. The influence or quality of the result is said to be optimized when the response of S/N is high. In addition to this, analysis of variance (ANOVA) was carried out to find out the most significant processing parameter. The primary concern of this analysis is to obtain optimum processing parameters for improved mechanical properties of Al6082 hybrid composites. The process parameters namely reinforcement content , stirs peed and stir time have a significant effect on the mechanical properties of both the hybrid composites [15, 16].To be very specific, the difference between the influences of all the parameters is quite minimal that is the reason why the values of the S/N ratio is showing minimal variations. But it should be understood that the idea is to check out all these which have more influence on the mechanical properties. In this scenario, the weight percentage of reinforcement plays a prominent role followed by stir speed and stir time indicating the mechanical properties.

Table 1. Chemical composition of Al6082 alloy

Element	Mg	Si	Fe	Mn	Cu	Cr	Al
Present, %	3.74	1.52	0.15	0.12	0.067	0.022	Bal.

Table 2. Basic properties of particulate reinforcement

Reinforcement	Density(g/cm^3)	Elastic modulus(GPa)	Tensile strength(MPa)	CTE($10^{-6}K^{-1}$)
B_4C_p	2.52	362	261	5.0
SiC_p	3.21	90	240	4.7

[DOI: 10.22068/ijmse.2507]

Table 3. Reinforcement combination and sample designation

SlNo	Hybrid composites	Designation
1	Al6082+4%Al_2SiO_5+4%B_4C	1,2,3
2	Al6082+4%Al_2SiO_5+8%B_4C	4,5,6
3	Al6082+4%Al_2SiO_5+12%B_4C	7,8,9

Table 4. Processing parameters and levels

Code	Parameter	Level		
		1	2	3
A	Stirring speed(rpm)	150	200	250
B	Stirring time(min)	4	8	12
C	Reinforcement content (wt %)	4	8	12

Table 5. Design matrix developed by ANOVA technique

Sl.No.	Al_2SiO_5 wt. %	B_4C wt.%	Stir speed	Stir time
1	4	4	150	4
2	4	4	200	8
3	4	4	250	12
4	4	8	150	8
5	4	8	200	12
6	4	8	250	4
7	4	12	150	12
8	4	12	150	12
9	4	12	200	4

3. RESULTS AND DISCUSSION

3.1. Microstructure

Cast microstructure of Al6082 based hybrid composites were studied using a scanning electron microscope (SEM) and energy-dispersive X-ray spectroscopy (EDS). Formation of microstructure, dispersion of multiple reinforcements, and their bonding with the matrix material was investigated using SEM which is quite important from a properties point of view.

3.1.1. Al6082/Al_2SiO_5/B_4C hybrid composite system

Fig.1 shows the SEM micrographs of Al6082 hybrid composite taken at different processing parameters such as varying B_4C particles content, stir speed and stir time. From the Figures, it can be observed that the microstructure consists of dendrites of α-aluminum, intermetallic compounds at the inter-dendritic spaces, and the presence of reinforcements. It can be also observed from Fig. 1 (b) that α - aluminum grain size for the A3 sample is lesser than that of other hybrid composite samples (A1, A5, and A7). From these low magnification micrographs, the dispersion of B_4C and Al_2SiO_5 particles is quite unclear. To check the particle dispersion and their bonding with the matrix, some micrographs were taken and presented in Fig. 2 (a). The SEM micrographs were taken for Al6082 hybrid composite with 4% Al_2SiO_5 and 12% B_4C particles for stirring time and stirring speed were 12 minutes and 150 rpm respectively. The microstructure consists of α-Al as the primary phase and both the reinforcements are visible in inter-dendritic regions. Both B_4C and Al_2SiO_5 particles were found and accumulated at the grain boundaries. Growing solid grains during solidification push the lightweight and small particles at the grain boundaries. Few particles are found to be trapped inside the grains and have a very good bonding with the matrix. Reinforcements are known to be potent sites for the nucleation of new grains especially the ones retained inside grains. The dispersion of B_4C and Al_2SiO_5 particles is roughly uniformly distributed throughout the matrix with good interface bonding. No visible clustering of reinforcements was observed for this sample indicating optimum processing parameters. As noted from SEM micrographs, very few Al_2SiO_5 particles were seen in the microstructure when compared to B_4C particles which are attributed to its low content in

[DOI: 10.22068/ijmse.2507]

the A7 sample. The chemical composition of the A7 sample was studied using EDS and obtained spectrum is presented in Fig. 2 (b). EDS showed the presence of major alloying elements such as Al, Mn, Fe, Si, B, and C which corresponds to Al6082 alloy, B_4C, and Al_2SiO_5 particles. Fig. 3 shows the presence of iron-rich intermetallic compounds like α-AlMnFeSi occupying interdendritic spaces along with reinforcements. As per previous literature viz., α-AlMnFeSi intermetallic compound formed in the present case has a close composition to that of $Al_{15}(FeMn)_3Si_2$ and a size of about ~10-20 µm [7]. EDS analysis was carried out at one of the interdendritic spaces and is shown in Fig. 2 (b). All the major elements corresponding to the α-AlMnFeSi intermetallic compound were observed in the EDS spectrum.

3.2. Effect of process parameters

The effect of process parameters is quite prominent on the microstructure and dispersion of multiple reinforcements of hybrid composites. With the increase in B_4C content to 12%, the grain size of α-Al grains is found to decrease which is quite evident from Fig. 1, 2 and 3. The α-Al grains are quite bigger for the A1 sample and it tends to decrease with the increase in B_4C contents. The refinement is attributed to the presence of multiple reinforcement combinations (B_4C/Al_2SiO_5) distributed uniformly throughout the matrix. During solidification, the reinforcements are pushed towards the solid/liquid interface which restricts the growth of α-Al grains. The grain refinement is mainly due to the disappearance of the dendritic structure due to the presence of a higher weight percentage of B_4C particles in the A7 sample.

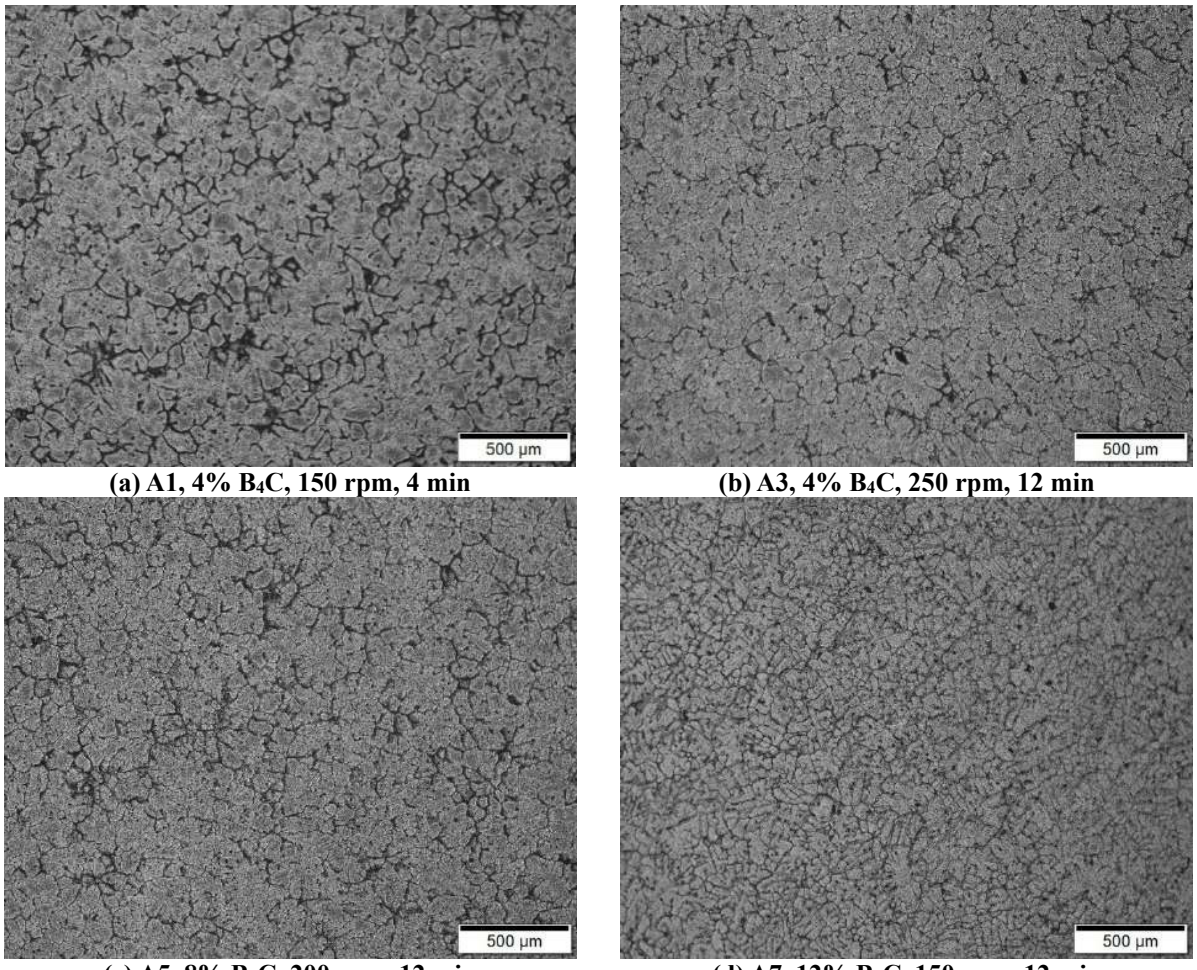

(a) A1, 4% B_4C, 150 rpm, 4 min **(b) A3, 4% B_4C, 250 rpm, 12 min**

(c) A5, 8% B_4C, 200 rpm, 12 min **(d) A7, 12% B_4C, 150 rpm, 12 min**

Fig. 1. Low magnification SEM micrographs of Al6082/Al_2SiO_5/B_4C hybrid composite system at different B_4C content, stir speed (rpm) and stir time (min).

[DOI: 10.22068/ijmse.2507]

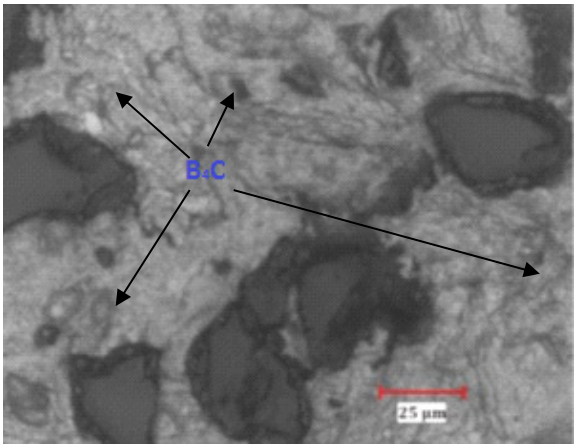

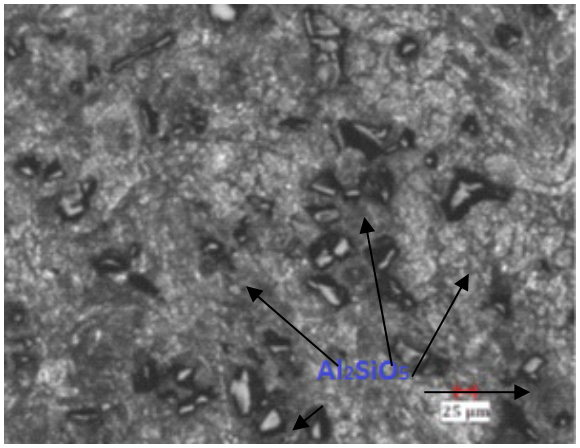

(a) A7, 12% B_4C, 150 rpm, 12 min

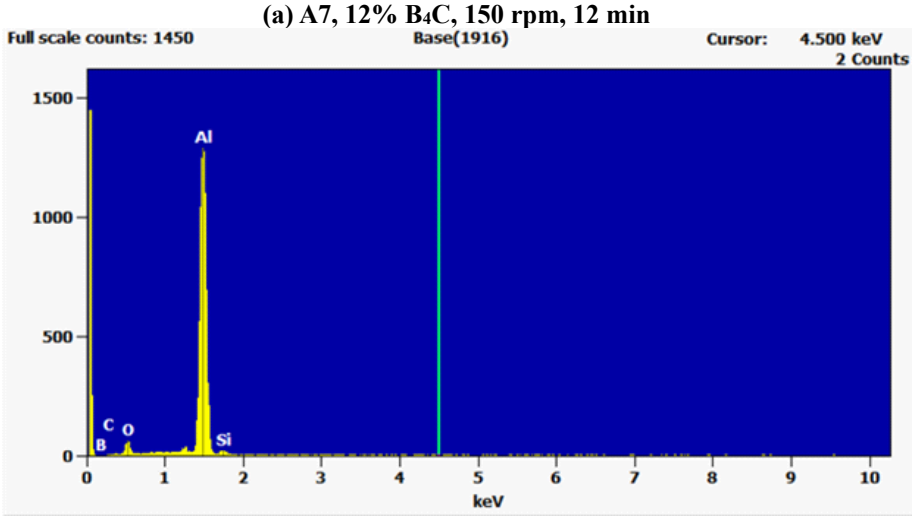

(b) EDS of A7 sample

Fig. 2. High magnification SEM micrographs and EDS of Al6082/Al_2SiO_5/B_4C hybrid composite system.

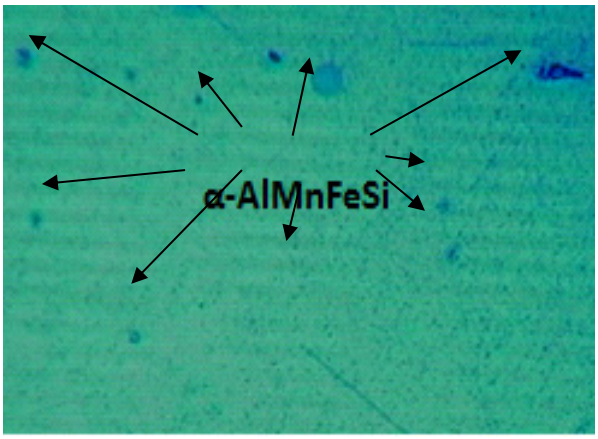

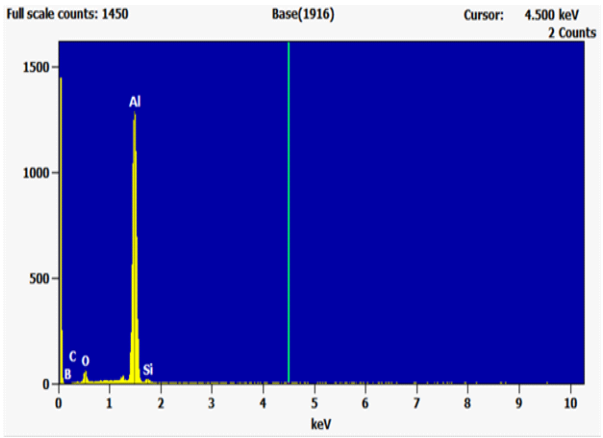

Fig. 3. SEM micrograph and EDS of A1 sample showing an α-AlMnFeSi intermetallic compound

These particles are entrapped in between the dendritic arms and pose a hindrance to their growth leading to modification in solidification pattern. A similar result has been reported by Ruirui et al [8], On the other hand, stir speed for the Al6082 hybrid composite system indicates an effect of particle size as well as particle content. Contrary to this the highest stir time of 12 minutes for Al6082/Al_2SiO_5/B_4C, composite systems showed good dispersion of reinforcements with

[DOI: 10.22068/ijmse.2507]

small grain sizes. An increase in stir time ensures uniform dispersion of reinforcements by giving enough time to disperse throughout the matrix without the formation of clusters. Overall, for all as cast Al6082 hybrid composites hardly any casting defects such as shrinkage, slag, entrapped gas pore, or reinforcement clusters are seen.

3.3. Tensile strength

It is well known that tensile strength is the resistance offered by a material against permanent deformation and is important from the mechanical design point of view. Especially when reinforcement is added to a metal matrix than the strength values change drastically. The strength depends largely on reinforcement content which in turn influences the grain size, dislocation density, and strain hardening. In the present work, the influence of stir cast processing parameters such as stir speed, stir time, and reinforcement weight percentage on tensile strength was tested by employing Taguchi's method. Using standard Taguchi's method with L9 orthogonal array, the tensile strength for different combinations of processing parameters was obtained and presented in this section. Here the tensile strength obtained is divided into three sections which concentrate on hybrid composite systems and the effects of processing parameters of hybrid composite systems.

3.3.1. Al6082/Al_2SiO_5/B_4C hybrid composite system

Table 6 shows Experimental result for tensile strength with calculated S/N ratios for Al6082/Al_2SiO_5/B_4C hybrid composite system and Table 7 shows the ultimate tensile strength values for the Al6082/Al_2SiO_5/B_4C hybrid composite system for a different combination of weight percentage of B_4C particles, stirring speed, and stir time followed by S/N ratio. Here for all cases from A1 to A9, the weight percentage of Al_2SiO_5 particles is fixed to 4 wt%. Strictly from the B_4C particles content point of view, it can be observed that with the increase in weight percentage up to 8 wt%, the tensile strength of Al6082 hybrid composites tends to increase. However, an increase in the weight percentage up to 12%; a marginal drop in the tensile strength is observed. The highest tensile strengthof192.81 MPa was obtained for a hybrid composite system with 8 wt% of B_4C particle content while the lowest tensile strength of 148.89 MPa was obtained for 4 wt% of B_4C particle content. The increment in tensile strength is about 29.49% for 8 wt% when compared to that of 4 wt% B_4C reinforced hybrid composite. The increase in tensile strength with the increase in B_4C particle content can be attributed to the fact that the stress experienced by the hybrid composite is quite different. In other words, the stress experienced by Al6082 hybrid composite with 8 wt% B_4C particle content is quite greater than that experienced by Al6082 hybrid composite with 4 wt% B_4C particle content. The increase in stress can be attributed to multiple factors like reduced grain size and an increase in the density of dislocations. The addition of B_4C and Al_2SiO_5particles has many effects on the microstructure of the Al6082 matrix which includes decrement in grain size, increase in dislocation density and higher plastic strain intensity which in turn affects the tensile strength of Al6082 hybrid composite [9, 10]. With the increase in wt% of B_4C particle content the grain size of the matrix tends to decrease due to two reasons, one is the new site for nucleation of new grains and the second is the restriction to the grain growth. During processing presence of B_4C and Al_2SiO_5 particles helps in nucleating in new grains while uniformly dispersed particles that are present adjacent to it restrict their growth. So with the increase in B_4C particle content, the grain size is expected to be lesser in Al6082 hybrid composite with 8 wt% B_4C particle content compared to Al6082 hybrid composite with 4 wt% B_4C particle content. The next contributor to the strength is the incorporation of dislocation plasticity arising due to the addition of B_4C and Al_2SiO_5particles [11]. When the reinforcements are added to the Al6082 matrix, the difference between the elastic and plastic properties gives rise to stress concentration at the interface during the tensile test. To maintain the displacement compatibility during the application of stress, the dislocations are generated at the interface. The interaction of dislocations with both B_4C and Al_2SiO_5particles decides the strength of hybrid composites. But again, this should not be confused with the strengthening caused by nucleation of dislocations during processing. Due to the difference in coefficient of thermal expansion mismatch between Al6082 matrix ($\sim 23.4\times10^{-6}$ K^{-1}) and B_4C ($\sim 4.5\times10^{-6}$ K^{-1}) and

[DOI: 10.22068/ijmse.2507]

Al_2SiO_5 (~5.2×10^{-6} K^{-1}) particles, the dislocations are generated in a matrix. The dislocation density increases with the increase in B_4C particle content which in turn is beneficial for improvement in tensile strength of Al6082 hybrid composite. In addition to this one more important strengthening mechanism comes into play which largely depends on the interface between B_4C, Al_2SiO_5particles, and Al6082 matrix. The load transfer from matrix to reinforcements is very crucial from a strength point of view which again largely depends upon the interfacial strength [12]. Due to good bonding between the Al6082 matrix and B_4C/Al_2SiO_5 particles the interface is quite strong and good enough to transfer the load from the matrix to these hard reinforcements. However, this largely depends on the dispersion of these reinforcements in the Al6082 matrix. From quantitative values, it is quite clear that the dispersion of B_4C particles is quite uniform for the Al6082 hybrid composite with 8 wt%. However, with an increase in B_4C particle content to 12 wt%, the clustering is quite pronounced due to which the interface between the clusters and matrix is weak. This led to a decrease in tensile strength values for hybrid composites with 12 wt% of B_4C particle content. Fig. 4 shows the Main effect plot for tensile strength of hybrid composite system.

Table 6. Experimental result for tensile strength with calculated S/N ratios for Al6082/Al_2SiO_5/B_4C hybrid composite system

Sl. No.	Wt. %	Stir speed (rpm)	Stir time (min)	Tensile strength (N/mm^2)	S/N ratio
A1	4	150	4	148.89	44.45
A2	4	200	8	167.52	44.48
A3	4	250	12	169.15	44.56
A4	8	150	8	182.05	45.20
A5	8	200	12	192.81	45.7
A6	8	250	4	172.71	44.74
A7	12	150	12	183.81	45.28
A8	12	200	4	171.81	44.70
A9	12	250	8	186.29	46.92

Table 7. Mean S/N ratio for tensile strength for Al6082/Al_2SiO_5/B_4C hybrid composite system

Level	Wt. %	Stir speed	Stir time
1	44.17	44.65	44.3
2	45.22	44.96	44.87
3	44.97	44.75	45.19
Delta	1.05	0.31	0.88
Rank	1	3	2

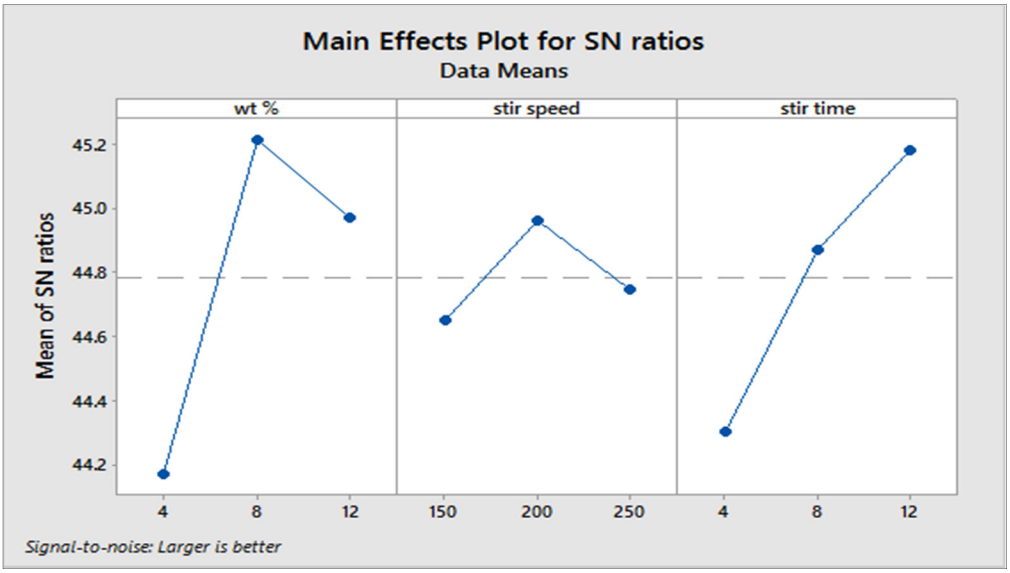

Fig. 4. Main effect plots for tensile strength for Al6082/Al_2SiO_5/B_4C hybrid composite system

[DOI: 10.22068/ijmse.2507]

4. FRACTOGRAPHIC ANALYSIS

Fractographic studies on both Al6082/Al_2SiO_5/B_4C hybrid composite systems after tensile test were carried out using SEM and the obtained results are shown in Fig. 5. The fracture analysis of both the hybrid composite systems with different particle weight percentages is presented below in two different sections.

4.1. Al6082/Al_2SiO_5/B_4C hybrid composite system

Fig. 5 (a) – (h) shows the SEM fractography of the Al6082/Al_2SiO_5/B_4C hybrid composite system with different weight percentages of B_4C particles taken after the tensile test. The SEM images of fractured hybrid composite samples of A1, A3, A5, and A7 were taken at both low and high magnification to understand the failure mechanisms. The hybrid composite samples A1 and A3 as shown in Fig. 5 (a) and (c) were found to be failed in a ductile manner however they also showed several regions of inter-dendritic cracking. Generally during solidification, the liquid metal cannot fill the inter-dendritic regions leaving behind micro- shrinkage. These micro-shrinkages can also be due to the presence of hydrogen gas dissolved in the molten metal. This hydrogen gas will precipitate out at the region where the last liquid solidifies leaving behind a micro-shrinkage [13, 14]. As evident by the images in Fig.5 (b) and (d), the appearance of micro-shrinkage is not spherical in nature and follows the dendrite shape. Such defects are the potent site for crack nucleation and when a tensile load is applied the cracks are initiated at this site.

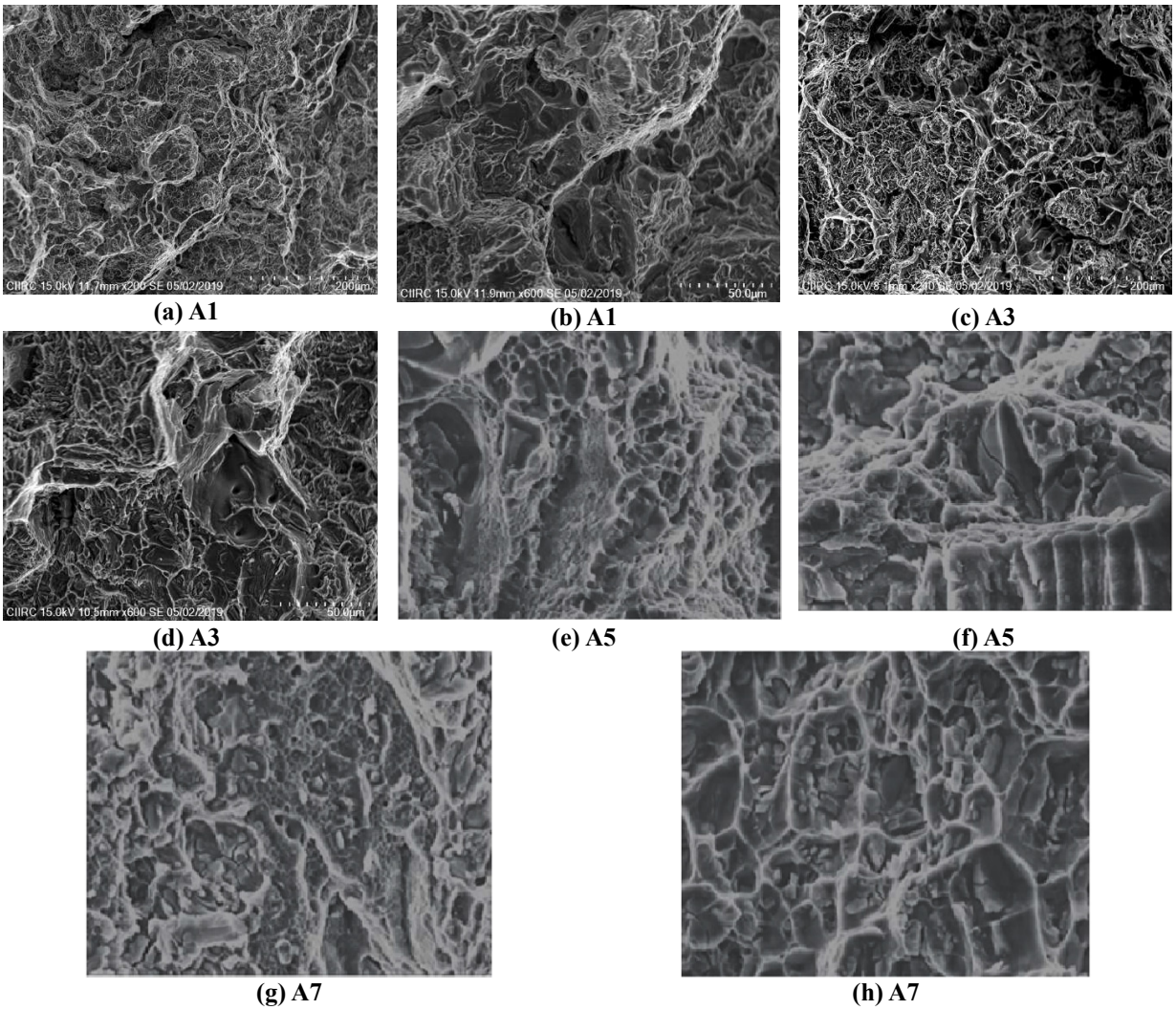

Fig. 5. Tensile fractured surfaces of Al6082/Al_2SiO_5/B_4C hybrid composite systems viewed using SEM at (a, c, e, g) low magnification and (b, d, f, h) high magnification

[DOI: 10.22068/ijmse.2507]

These cracks will propagate into such defects regions ultimately leading to the failure of the composite sample. On the other hand, the failure of hybrid composite samples A5 and A7 is found to be composed of both inter-dendritic cracking as well as cleavage fracture of B_4C particles (see Fig. 5 (e) and (g)). Cleavage fracture of both Al_2SiO_5 and B_4C particles are seen in the matrix especially in the images Fig.5 (f) and (h). The cleavage fracture of both the reinforcements explains that bonding between them and the Al6082 matrix material is very good. Generally, when the interfacial bonding between matrix and reinforcement is good then particle fracture is observed rather than particle debonding. The obtained results of fracture after the tensile test are in good agreement with the previously published articles [17, 18]. So, in the present case, the hybrid composite samples A5 and A7 with high B_4C content of 8 and 12 wt% showed particle fracture indicating high interfacial strength compared to particle strength.

4.2. High cycle fatigue test

The fatigue life of any material/component is the ability to resist the number of stress cycles before tending to failure or fracture and widely depends particularly on the material characteristics, geometry, and service conditions (environment). The material characteristics depend upon the microstructure which is being influenced by its phases and processing parameter. In the present work, the influence of stir cast processing parameters such as stir speed, stir time, and reinforcement weight percentage on the number of cycles for failure was tested by employing Taguchi's method. Using standard Taguchi's method with L9 orthogonal array, the number of cycles for failure for different combinations of processing parameters was obtained and presented in this section. Here the number of cycles for failure obtained is divided into three sections which concentrate on two different hybrid composite systems and one of the effects of processing parameters for both hybrid composite systems.

4.2.1. Al6082/Al_2SiO_5/B_4C hybrid composite system

Table 8 shows the number of cycles to failure values for Al6082/Al_2SiO_5/B_4C hybrid composite system for a different combination of weight percentage of B_4C particles, stir speed, and stir time followed by S/N ratio.

In conventional fatigue tests, the run-outs are usually declared at 107 cycles but in the present case, the fatigue life is found to be near 109 cycles. The different fatigue lives for these samples indicate the effect of different processing parameters. Strictly from the B_4C particles content point of view, it can be observed that with the increase in weight percentage up to 12 wt%, the fatigue life of Al6082 hybrid composites tends to increase.

Hybrid composite sample A5 showed the highest number of cycles to failure (9935923) while hybrid composite sample A1 showed the lowest number of cycles to failure (7793918). The increase in B_4C particles content had a positive influence on the fatigue performance of the hybrid composite samples. However, with a further increase in B_4C particle content to 12 wt% the number of cycles to failure increased marginally. The possibility of lower fatigue life for composites with 4 wt% B_4C particles content can be attributed to various factors. Out of all, the main factor affecting fatigue life in these samples is the presence of micro-shrinkage.

Table 8. Cycles to failure for Al6082/Al_2SiO_5/B_4C hybrid composite system

Sl. No.	P_{max}	P_{min}	Frequency	No. of cycles to failure
A1	7.290 kN	0.729 kN	25 Hz	7793918
A2	7.290 kN	0.729 kN	25 Hz	8366426
A3	7.290 kN	0.729 kN	25 Hz	8059076
A4	7.290 kN	0.729 kN	25 Hz	9840979
A5	7.290 kN	0.729 kN	25 Hz	9935923
A6	7.290 kN	0.729 kN	25 Hz	9814564
A7	7.290 kN	0.729 kN	25 Hz	9859431
A8	7.290 kN	0.729 kN	25 Hz	9901256
A9	7.290 kN	0.729 kN	25 Hz	9916552

[DOI: 10.22068/ijmse.2507]

The presence of such casting-related defects can be a potential site for early fatigue crack initiation and thus result in reduced fatigue life Also, the possibility of clustering of B_4C/Al_2SiO_5 could be a possible detrimental reason for reduced fatigue life. If the processing conditions are not optimum then there is a very high chance of clustering of B_4C particles [19]. Clustering of the B_4C particles leads to poor interfacial bonding with that of Al6082 matrix which is prone to de-bond easily and causes a reduction in fatigue life for this particular B_4C particles content-based hybrid composite sample (4 wt %).

On the other hand, the fatigue life of hybrid composites has been found to increase with the increase in B_4C particles content. It is attributed to the crack deflection by the hard B_4C particles [20].

4.3. Numerical analysis of Al6082/Al_2SiO_5/B_4C hybrid composite system

The numerical analysis of Al6082/Al_2SiO_5/B_4C hybrid composite system for different combinations of weight percentages of B_4C particles was analyzed and is presented in Fig.6. The stress plot for maximum principal stress condition is presented in Fig. 6 (a) and the fatigue life plot is given in Fig. 6 (b) – (d).

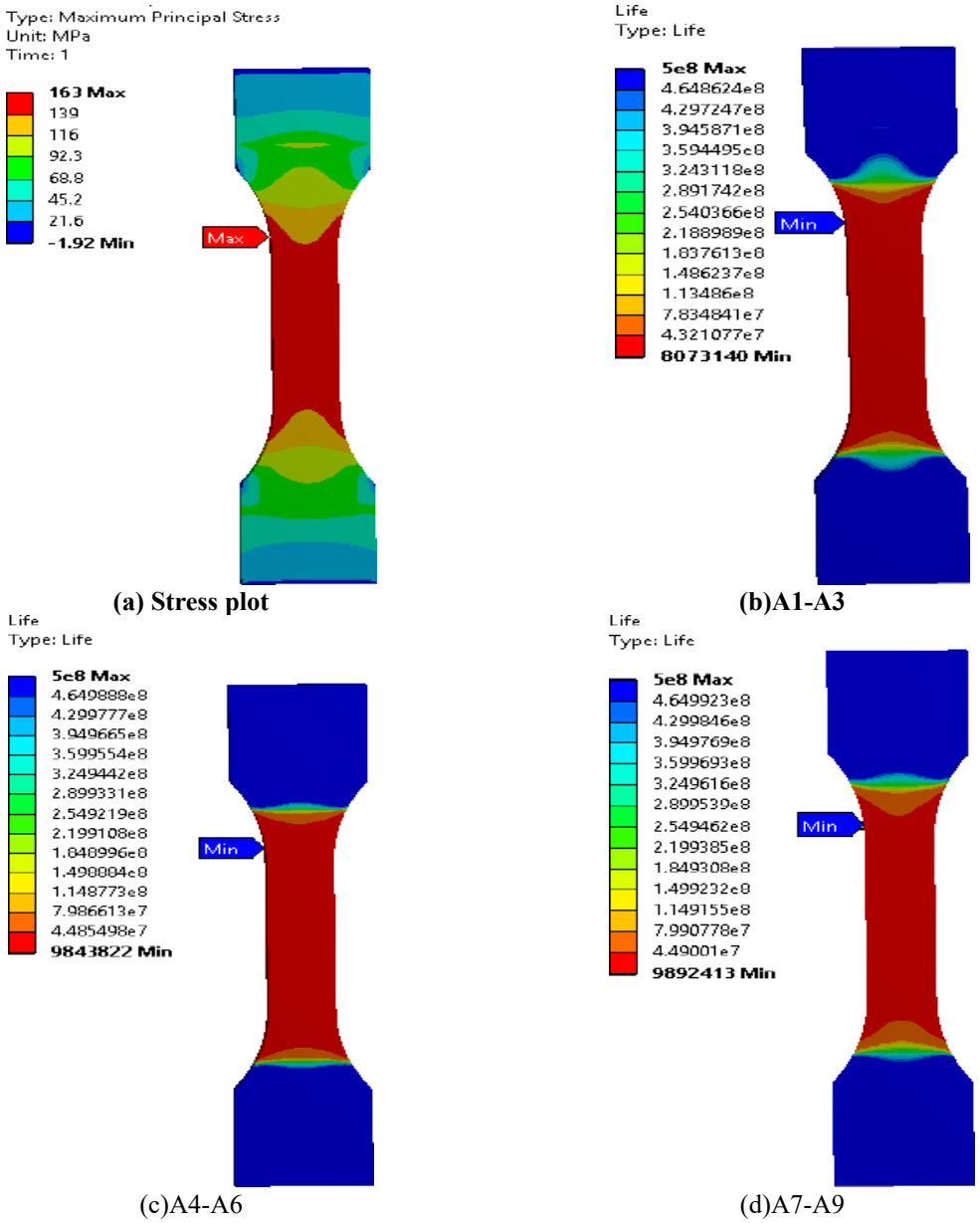

Fig. 6. Stress and fatigue life plot of Al6082/Al_2SiO_5/B_4C hybrid composite system

[DOI: 10.22068/ijmse.2507]

Stress analysis of samples is done via observing the stress distribution in the model of the fatigue specimen. One can see from Fig. 6 (a) that most of the stress is concentrated at the reduced cross-section of the fatigue specimen. As shown in Fig. 6 (b) – (d), for samples A1 to A3 the number of cycles for failure is about 8073140, for samples A4 to A6 it is 9843822 while for A7 to A9 it is 9892413. With the increase in B_4C weight percentage the required number of cycles to failure is found to be increasing which explains that the fatigue life is increasing. The number of cycles for failure obtained from the numerical analysis is quite comparable with that obtained from experimentation.

4.4. Fractographic analysis

Fracture surfaces of Al6082/Al_2SiO_5/B_4C and Al6082/Al_2SiO_5/Al_2O_3hybrid composite systems for different combinations of weight percentage of B_4C particles were analyzed after the high cycle fatigue test and are presented in Fig.7.The fracture surface of Al6082/Al_2SiO_5/B_4C hybrid composite system for different combinations of weight percentages of B_4C particles was analyzed and is presented in Fig. To start with, Fig. 7 (a, b) shows the low and high magnification SEM micrographs of the fracture surface of the Al6082 hybrid composite with 4%B_4C particle content. From the micrographs, it is quite clear that the micro-shrinkage pores present in the sample are the major reason for the failure of the composite sample. The crack is initiated through these micro-shrinkage pores under the action of fatigue loading. On the other hand, Fig. 7 (c, d) & (e, f) shows the low and high magnification SEM micrographs of a fracture surface of Al6082 hybrid composite with 8%and 12% B_4C particle content and it also shows a similar reason for failure. Microstructural heterogeneities like porosity, intermetallic compounds, and oxide inclusions affect the fatigue life and develop favorable conditions for crack initiation and propagation [21, 22]. In all the cases the main reason for failure can be identified as micro-shrinkage pores.

4.5. Fatigue Crack Growth Test

Fatigue crack propagation or fatigue crack growth tests were performed on compact tensions specimens of both Al6082 hybrid composite systems. It is well known that the reinforcement content and its type, processing conditions, and matrix properties have a large influence on fatigue crack propagation. In particular, the interaction between the reinforcement and propagating fatigue crack largely dictates the composite response towards fatigue crack behavior. Keeping this in mind, this section presents the fatigue crack response of two Al6082 hybrid composite systems reinforced with different reinforcements.

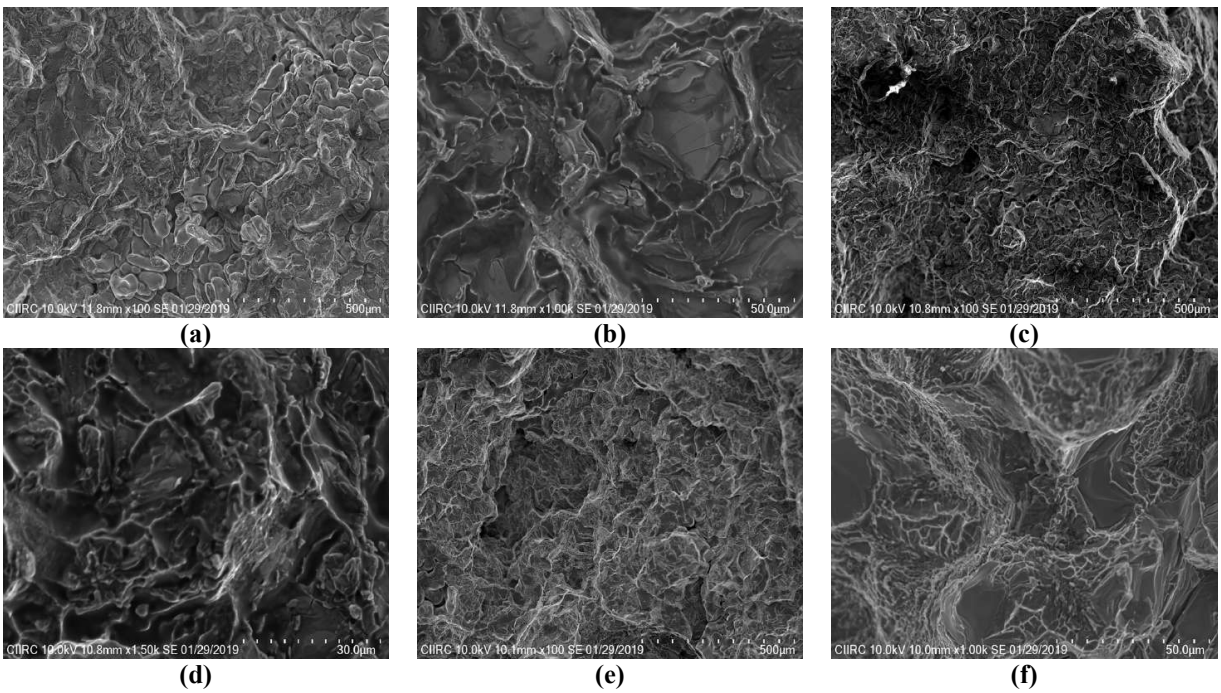

Fig. 7. Fracture analysis ofAl6082/Al_2SiO_5/B_4C hybrid composite system With (a, b) 4%, (c, d) 8% and (e, f) 12% B_4C content

[DOI: 10.22068/ijmse.2507]

4.5.1. Al6082/Al_2SiO_5/B_4C hybrid composite system

Table 9 shows the number of cycles for failure values for Al6082/Al_2SiO_5/B_4C hybrid composite system for different combinations of weight percentage of B_4C particles, stirring speed, and stir time followed by S/N ratio. It can be seen from Table 9 that, with the increase in B_4C particle content the resistance to fatigue fracture is improved. The higher content of B_4C particles generally acts as an effective barrier for fatigue crack growth. This result is well supported by the work done by Li et al [23] on fatigue crack growth studies on AlSiMg/SiC composites. Compared to unreinforced alloy, the composite showed better fatigue crack growth resistance due to the presence of SiC particles. In the present case, the B_4C particles play an important role by acting as obstacles to crack propagation. There are two scenarios when a crack approaches the B_4C particles, one is either crack cuts through the particle and the second is it bypasses the particle completely. Owing to strong interfacial bonding strength between B_4C particles and the Al6082 matrix, the particle fracture due to fatigue crack can be ruled out or said it is minimal. In such a case the fatigue crack is deflected and one can expect a local reduction in the crack driving force. Due to which the applied maximum and minimum stress intensity factors are expected to be effectively reduced. Thus, the crack tends to grow around the B_4C particles and uniform dispersion of these particles can lead to a weaker fracture path [24, 25]. This is the reason why the number of cycles to failure for hybrid composites with higher B4C particle content (12%) is larger than that of hybrid composites with lower B_4C particle content (4%). Further, the addition of B_4C particles strengthens the Al6082 matrix material due to which one can expect a reduction in crack tip opening displacement causing lowering of plastic strain ahead of the crack tip.

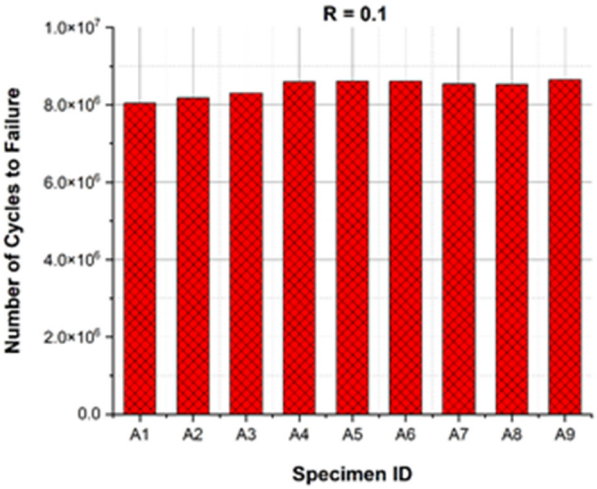

Fig. 8. Fatigue life distribution

4.6. Numerical analysis of Al6082/Al_2SiO_5/B_4C hybrid composite system

The numerical analysis of Al6082/Al_2SiO_5/B_4C hybrid composite system for a different combination of weight percentages of B_4C particles was analyzed and is presented in Fig. 8. The analysis started for the sample having an initial crack length of 15.1 mm and was allowed to grow up to the final crack length of 22.85 mm. As shown in Fig.9 (a) – (c), for samples A1 to A3 the number of cycles for failure is about 8168159, for samples A4 to A6 it is 8607698 while for A7 to A9 it is 8571495. With the increase inB_4C weight percentage the number of cycles to failure is found to be increasing up to 8% B_4C content which indicates that the fatigue life is increasing. However, beyond 8% B_4C content the required number of cycles to failure is found to be decreasing which indicates that the fatigue life is decreasing. The number of cycles for failure obtained from the numerical analysis is quite comparable with that obtained from experimentation.

Table 9. Cycles to failure for Al6082/Al_2SiO_5/B_4C hybrid composite system

Sl No.	Specimen ID	P_{max}	P_{min}	No. of cycles to failure
2	A2	20 kN	2 kN	8036858
3	A3	20 kN	2 kN	8168974
4	A4	20 kN	2 kN	8298645
5	A5	20 kN	2 kN	8596857
6	A6	20 kN	2 kN	8612589
7	A7	20 kN	2 kN	8613648
8	A8	20 kN	2 kN	8541789
9	A9	20 kN	2 kN	8521458

[DOI: 10.22068/ijmse.2507]

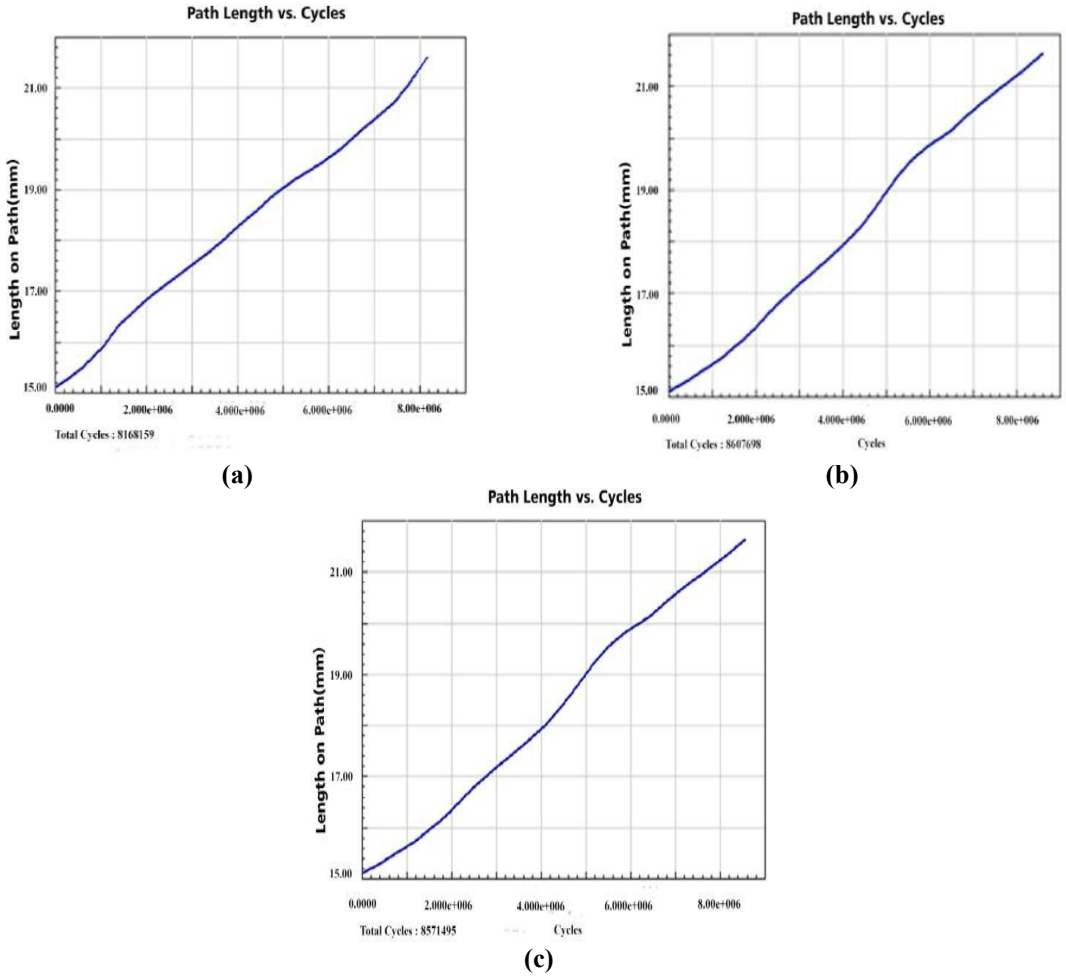

Fig. 9. Fatigue crack growth analysis from Al6082/Al_2SiO_5/B_4C hybrid composite system

4.7. Fractographic analysis

Fracture surfaces of Al6082/Al_2SiO_5/B_4C hybrid composite systems for a different combination of weight percentages of B_4C particles were analyzed after fatigue crack growth test on CT specimen and are presented in Fig.10.

The fracture surface of Al6082/Al_2SiO_5/B_4C hybrid composite system for a different combination of weight percentages of B_4C particles was analyzed and is presented in Fig. 10. To start with, Fig. 10 (a, b) shows the low and high magnification SEM micrographs of a fracture surface of Al6082 hybrid composite with 4% B_4C particle content. From the micrographs, it is quite clear that the micro-shrinkage pores present in the sample are the major reason for the failure of the composite sample. However, a high magnification shows a crack propagating in the surface but a lot of deflection in the crack path can be seen.

On the other hand, Fig.10 (c, d) shows the low and high magnification SEM micrographs of the fracture surface of Al6082 hybrid composite with 12% B_4C particle content shows a similar reason for failure. Here the crack is found to be propagating along with the network of micro-shrinkage pores. In all the cases the main reason for failure can be identified as micro-shrinkage pores.

5. CONCLUSIONS

An increase in tensile strength of both the hybrid composite system was attributed to the decrease in grain size, increase in dislocation density, and higher plastic strain intensity. ANOVA analysis showed that combination of that 8 wt. % and stir time of 12 minutes were optimum for obtaining high tensile strength in both the hybrid composite system. Tensile fracture studies of both the hybrid composite system showed the failure of samples in a ductile manner along with inter-dendritic cracking.

[DOI: 10.22068/ijmse.2507]

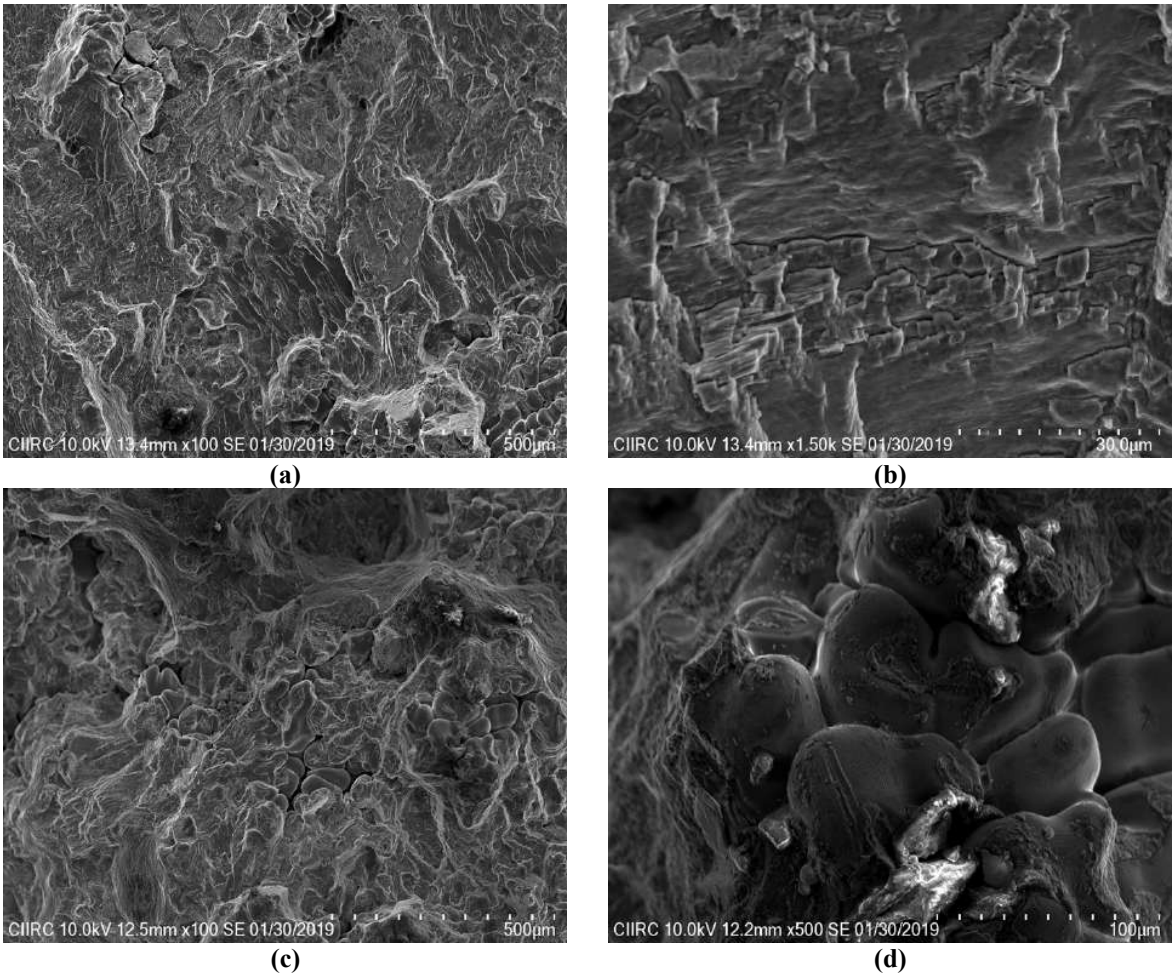

Fig. 10. Fracture analysis ofAl6082/Al_2SiO_5/B_4C hybrid composite system with (a, b) 4% and (c, d) 12% B_4C content

Three-point bend tests revealed the segregation of intermetallic compounds in line with the literature from Al6082 matrix and alloying elements helped in the nucleation of cracks at these inter-dendritic regions in both the hybrid composite system. High cycle fatigue tests showed that an increase in B_4C content in hybrid composite systems had a positive influence on the fatigue performance of the hybrid composite samples. The numerical analysis of both the hybrid composite system showed that the number of cycles for failure obtained was quite comparable with that obtained from experimentation. The main reason for failure was identified as micro-shrinkage pores that acted as a crack initiating and propagation along the network of micro-shrinkage pores causing failure. Overall, this work showed that using the Taguchi technique along with ANOVA, optimum processing parameters can be obtained for achieving improved mechanical properties for Al6082 hybrid composite systems.

6. REFERENCES

[1] Krishna, K Chawla, Composite Materials Science and Engineering, Fourth Edition, Springer Nature, Switzerland, 2019, 18-63.

[2] Autar, K Kaw, Mechanics of Composite Materials, CRC Press, 1997, 1-60.

[3] Hull, D and Clyne, T.W., An Introduction to Composite Materials, Second Edition, Cambridge University Press, Cambridge, 1996, 1-45.

[4] Sabu Thomas, Kuruvilla Joseph, S.K. Malhotra, KoichiGoda, M.S. Sreekala, Polymer composites, Volume 1, WILEY – VCH, USA, 2013, 6-39.

[5] Brian Cantor, Fionn. P.E. Dunne, Ian C Stone, Metal and Ceramic Matrix composites, First Edition, CRC Press, Boca Raton, 2003, 50-63.

[DOI: 10.22068/ijmse.2507]

[6] Subra Suresh, Fundamentals of Metal-Matrix Composites, First Edition, Butterworth- Heinemann, USA, 2013, 129-191.

[7] Hemanth, J, "Fracture toughness and wear resistance of aluminum-boron particulate composites cast using metallic and non-metallic chills", Mater. Des., 2002, 23, 41-50.

[8] Ruirui, W, Zheng, Y, Qiushu, L, "Microstructure and mechanical properties of 7075 Al alloy based composites with Al_2O_3 nanoparticles", Int. J. Cast Metal Res., 2017, 30, 337-340.

[9] Arsenault, R.J., Fisher, R.M., "Microstructure of fiber and particulate SiC in 6061 Al Composites", Scr. Mater., 1983, 17, 67-71.

[10] Arsenault, R.J., "The strengthening of aluminum alloy 6061 by fiber and platelet silicon Carbide", Mater. Sci. Eng., 1984, 64, 171-181.

[11] Hao, S, Xie, J, "Tensile properties and strengthening mechanisms of SiCp-reinforced aluminum matrix composites as a function of relative particle size ratio", J. Mater. Res., 2013, 28 2047-2055.

[12] Gao, X, Yue, H, Guo, E, Zhang, H, Lin, X, Yao, L, Wang, B, "Preparation and tensile properties of homogeneously dispersed graphene reinforced aluminum matrix composites", Mater. Des., 2016, 94, 54-60.

[13] Stefanescu, D.M., Ruxanda, R. Solidification Structures of Aluminum Alloys in ASM Handbook Volume 9, Metallography and Microstructures, George F. Vander Voort Ed., 2004.

[14] Stefanescu, D.M., Science and Engineering of Casting Solidification, Second Edition, Springer-Verlag US, 2009, 1-15.

[15] Puneeth, N, Satheesh, J, Naveen, G.J., Mohan, N, Litton Bhandari, Kiran, G, "Development and investigation on elastic-plastic fracture analysis of Al6082 Reinforced alumina/aluminum silicate MMCs using Taguchi approach", Mater. Today: Proc., 2020, 27, 2243-2248.

[16] Puneeth, N, Satheesh, J, Koti, V, Praveennath Koppad, G, Akbarpour, M.R., Naveen, G.J., "Application of Taguchi's method to study the effect of processing Parameters of Al6082/B_4C/Al_2SiO_5 hybrid composites on mechanical properties", Mater. Res. Express, 2019, 6, 1-22.

[17] Show, B.K., Mondal, D.K., Biswas, K., Maity, J, "Development of a novel 6351 Al- (Al_4SiC_4+SiC) hybrid composite with enhanced mechanical properties", Mater. Sci. Eng. A, 2013,579, 136-149.

[18] Trinh, P.V., Lee, J, Minh, P.N., Phuong, D.D., Hong, S.H., "Effect of oxidation of SiC particles on mechanical properties and wear behavior of SiCp/Al6061 composites", J. Alloys Compd., 2018,769, 282-292.

[19] Mahadevan, K, Raghukandan, K, Senthilvelan, T, Pai, B.C., Pillai, U.T.S., "Investigations on the high cycle fatigue behavior of stir cast AA 6061-SiCp composites, J. Mater. Sci., 2006, 41, 5548-5555.

[20] Chen, Z.Z., Tokaji, K, Minagi, A, "Particle size dependence of fatigue crack propagation in SiC particulate-reinforced aluminium alloy composites", J. Mater. Sci., 2001, 36, 4893-4902.

[21] Hemanth, J, "Fabrication and mechanical properties (strength and fracture toughness) of chilled aluminum alloy–glass particulate composite," Mater. Sci. Eng. A, 2001, 318, 277-284.

[22] Perez Ipina, J.E., Yawny, A.A., Stuke, R, Gonzalez Oliver, C., "Fracture toughness in Metal matrix composites," Mat. Res., 2000, 3, 74-78.

[23] Li, W, Liang, H, Chen, J, Zhu, S.Q., Chen, Y.L., "Effect of SiC particles on fatigue crack growth behavior of SiC particulate-reinforced Al-Si alloy composites produced by spray forming," J.mspro., 2014, 3, 1694 –1699.

[24] Milan, M.T., Bowen, P., "Fatigue Crack Growth Resistance of SiCp Reinforced Al Alloys: Effects of Particle Size, Particle Volume Fraction, and Matrix Strength." J. Mater. Eng. Perform, 2004, 13, 612-618.

[25] Gasem, Z.M., "Fatigue crack growth behavior in powder-metallurgy 6061 aluminum alloy reinforced with submicron Al_2O_3 particulates." Compos. B. Eng., 2012, 43, 3020- 3025.

[DOI: 10.22068/ijmse.2507]